

Robust High-Transparency Haptic Exploration for Dexterous Telemanipulation

Keyhan Kouhkiloui Babarahmati, Carlo Tiseo, Quentin Rouxel, Zhibin Li, and Michael Mistry

Abstract—Robot teleoperation has been proposed as a solution to perform complex tasks in dangerous or remote environments. Teleoperation dexterity is not yet sufficient to enable effective interaction control, even in short-range operation, and low communication delays between the slave and the master. This manuscript explores the development of a haptic teleoperation setup that relies upon a recently proposed passive impedance controller, called Fractal Impedance Controller (FIC). The controller has a state-dependent impedance which enables to tune the slave task accuracy. The proposed controller has been compared with a similar setup using a traditional impedance controller. The results show that the proposed control architecture has higher transparency of interaction compared to the impedance controller. A preliminary study on the ability of an expert user to perform dexterous tasks has been conducted maintaining constant controller parameters. The tasks included opening an electrical box, driving a pile in the sand, pushing a ball on rough terrain, moving a sponge in an obstacle course, and pushing an E-stop button. The results show that the proposed method can complete all the task while the impedance controller on the slave could not. Furthermore, the FIC enables a shorter completion time on the tasks completed that have been also completed from the traditional impedance controller (pushing a ball, moving the sponge, and pushing E-Stop).

I. INTRODUCTION

Exploration robots have already been deployed in multiple space missions both on Mars and the Moon. However, the current technology still offers limited manipulability. The development of more dexterous teleoperation platforms can help the deployment of robot-driven exploratory missions which can relieve the astronauts from the most dangerous tasks. This is the motivation of the METERON (Multi-Purpose End-To-End Robotic Operation Network) project [1], [2] from the European Space Agency (ESA) that aims to demonstrate the operational ability to teleoperated planetary robots from in-orbit crewed station. For example, on Mars, ancient potential life signs are expected to be found in sedimentary layers. Tasks such as collect and analyse on-site geological samples, assemble and build planetary structures are strongly demanded. Drilling, digging and collecting specific ground samples for analysis on complex surfaces of various mechanical properties will require dexterous manipulations with human supervision and low signal latency (e.g. from surface base) for dealing with complex situations. Similar capabilities are also strongly sought on earth where hazardous environments prevent direct human intervention

Keyhan Kouhkiloui Babarahmati, Carlo Tiseo, Quentin Rouxel, Zhibin Li, and Michael Mistry are with the School of Informatics, University of Edinburgh. Email: keyhan.kouhkiloui@ed.ac.uk, ctiseo@ed.ac.uk, quentin.rouxel@ed.ac.uk, zhibin.li@ed.ac.uk, mmistry@inf.ed.ac.uk

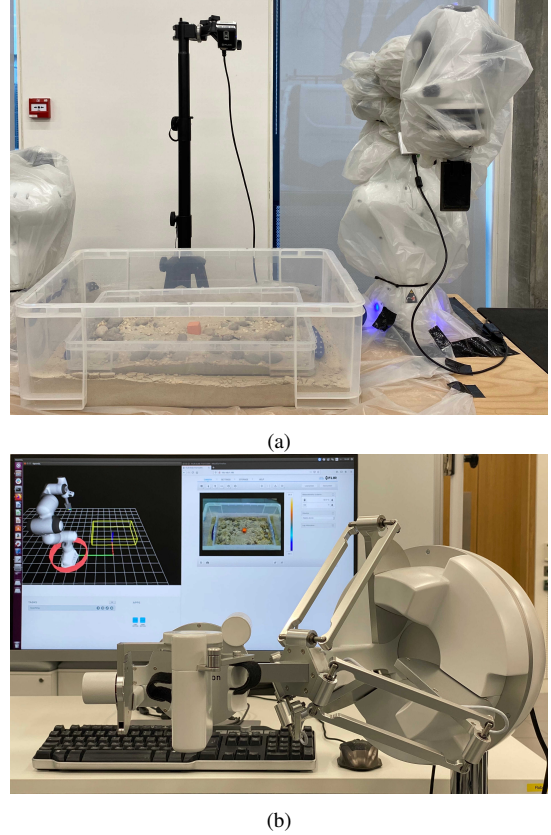


Fig. 1. Experimental setup: (a) Slave (Panda 7-DoF Manipulator Arm) and Simulated Environment; (b) Master Setup: Sigma.7 and GUI.

such as nuclear decommissioning or underwater robotics. These delicate and dexterous tasks involving establishing and breaking multiple contacts with the environment are still challenging to model or fully automate using autonomous robots. Therefore, a lot of research effort is still put into studying human-in-the-loop guidance and supervision based on multimodal sensory interface, especially the haptic feedback for highly accurate manipulation tasks.

Robots can provide a solution for reducing the intrinsic risk associated with extreme and hazardous environments. However, they are not yet able to meet the robustness and dexterity of interaction required even by task that are mundane for human operators. Port-Hamiltonian controllers (i.e., impedance and admittance, [3], [4]) have been identified as a good candidate to enhance the interaction capabilities of robots deployed in such environments. These controllers are designed to drive the robot as an equivalent mass-spring-damper system. However, the coupling of the robot

II. CONTROL ARCHITECTURE

The proposed method for bilateral haptic manipulation, Figure 2, has two physical interfaces. The first interface is between the user and the master. It is controlled using an admittance controller that mimics the interaction dynamics at the robot end-effector. The second interface is between the slave and the environment, where the system behaves as an impedance mimicking the user input acquired by the master device. Therefore, higher is the transparency of the intermediary (i.e., teleoperation system) higher is the dexterity of interaction [22]. An ideal teleoperation transparency is when the system set-up acts as an identity transformation with infinite bandwidth (i.e, there is no intermediary between the user and the environment).

The proposed architecture aims at improving the system transparency by using a Fractal Impedance controller (FIC) [21] instead of the classic impedance controller in the slave (IC). Appendix I gives a more detailed overview to the FICs. Within the context of this paper, the subscripts S and M stand for Slave and Master, respectively. We also proposed the introduction of an FIC for Safety and Haptic Enhancement (FIC_{SHE}), which will be used in this work as a safety mechanism on the master device. The master device is controlled using an admittance controller (A_M), using an identity matrix as gain and includes the Sigma.7 gravity compensation. The master position error (x_M) is the input to P controller (K_c) generating a virtual force (f_v) on the slave's end-effector whenever the button of the master's gripper is not pressed. In the case where the user activates the gripper button, the slave's desired position (x_{sd}) is recorded. It will be continuously updated by adding the current master position to the initial value of x_{sd} until the gripper is released. In other words, $x_{sd}(t_{\text{release}}) = x_{sd}(t_{\text{activation}}) + x_M(t_{\text{release}})$.

Despite these control modality being useful in dexterous fine interaction, they are not easy to use for large movements. Therefore, we have implemented a keyboard based input through a GUI to modify the desired pose of the FICs ($x_{sd}(t) = x_{\text{GUI},d}(t)$), which will autonomously drive the robot to the desired pose. Finally, the GUI is also used to provide the visual feedback from the FLIR AX-8 camera.

A. Master's Controllers

The master joint torque command is determined by the summation of the admittance controller (A_M) and the FIC_{SHE}.

$$\begin{aligned}\tau_M &= J_M^T(\text{FIC}_{\text{SHE}}) + A_M = \\ &= J_M^T(K_M(\tilde{x})\tilde{x}_M - D_M\dot{x}_M) + g_M(q_M) + J_M^T F_{\text{FB}}\end{aligned}\quad (1)$$

where D_M is the (diagonal) damping gain and $g_M(q)$ is the gravity compensation term and q_M are the joint configurations.

B. Slave's Controllers

The Slave's controller is the combination of the P controller, the FICs, Slave's inverse dynamics compensation and

null-space controller

$$\begin{aligned}\tau_{\text{FICs}} &= J_S^T K_c x_M + J_S^T (\text{FIC}_S) + J_S^T h_S(q_S, \dot{q}_S) \\ &+ (I - J_S^T (M_S^{-1} J_S^T (J_S M_S^{-1} J_S^T)^{-1}))^T \tau_{\text{Snull}} \\ &+ g_S(q_S) \\ &= J_S^T (K_c x_M + K_S(\tilde{x})\tilde{x}_S - D_S\dot{x}_S + h_S(q_S, \dot{q}_S)) \\ &+ (I - J_S^T (M_S^{-1} J_S^T (J_S M_S^{-1} J_S^T)^{-1}))^T \tau_{\text{Snull}} \\ &+ g_S(q_S)\end{aligned}\quad (2)$$

where J_S is the end-effector Jacobian, M_S is the inertia matrix and τ_{Snull} is the null space torque. $h_S(q_S) = \Lambda_S(q_S)(\ddot{x}_S + J_S M_S^{-1} C_S(q_S, \dot{q}_S)\dot{q}_S - \ddot{J}_S \dot{q}_S)$ is the inverse dynamics compensation. $\Lambda_S(q) = (J_S M_S^{-1} J_S^T)^{-1}$ is the task-space inertia matrix and $C_S(q, \dot{q})$ is Coriolis's matrix. $g_S(q_S)$ is the gravity compensation vector in joint-space. The following equation presents the wrench calculation in our proposed bilateral telemanipulation.

C. Slave's Impedance Controller

The impedance controller law is similar to the FICS control law. However, the fractal attractor and the non-linear impedance profile have been removed. While it has been kept the constant stiffness and the damping.

$$\begin{aligned}\tau_{\text{FICs}} &= J_S^T K_c x_M + J_S^T (\text{IC}_S) + J_S^T h_S(q_S, \dot{q}_S) \\ &+ (I - J_S^T (M_S^{-1} J_S^T (J_S M_S^{-1} J_S^T)^{-1}))^T \tau_{\text{Snull}} \\ &+ g_S(q_S) \\ &= J_S^T (K_c x_M + K_{\text{Sc}}\tilde{x}_S - D_S\dot{x}_S + h_S(q_S, \dot{q}_S)) \\ &+ (I - J_S^T (M_S^{-1} J_S^T (J_S M_S^{-1} J_S^T)^{-1}))^T \tau_{\text{Snull}} \\ &+ g_S(q_S)\end{aligned}\quad (3)$$

where K_{Sc} is the constant component in $K_S(\tilde{x})$.

III. EXPERIMENTAL VALIDATION

The comparison between the proposed method and the fractal impedance controller has been conducted from the perspective of the user, as shown in Figure 2. To evaluate transparency we analysed admittance characteristics of the set-up; thus, a spectral analysis has been conducted considering the force signals measured on the slave's end-effector as input and the velocity produced on the master as output of the system.

The two following experiments were performed:

- i) *System impulsive response*: Force impulse were applied to the slave's end-effector using an hammer and the master's end-effector was not hold.
- ii) *Interaction effect on system response*: The user drove the robot in contact with each of the 5 objects depicted

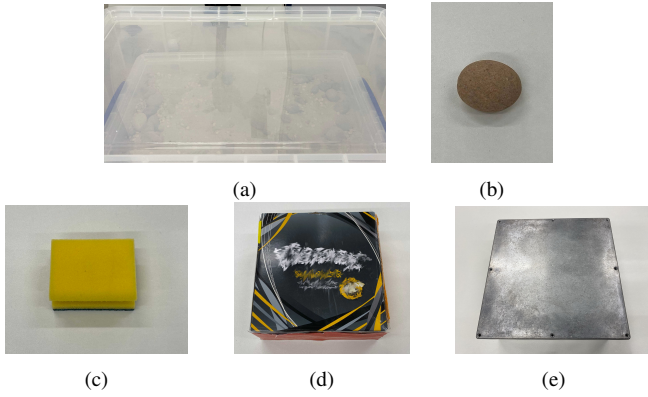


Fig. 3. (a) Obj 1: It is the lid of the bigger plastic box in Figure 1a. (b) Obj 2: Small rock. (c) Obj 3: Kitchen sponge (d) Obj 4: Tissue paper box (e) Obj 5: Metal box.

in Figure 3 before releasing his hold on the master's end-effector. The objects' dynamic changes from stiff to compliant enabling to evaluate the controllers' robustness to the coupling effects, which occurs in impedance controllers.

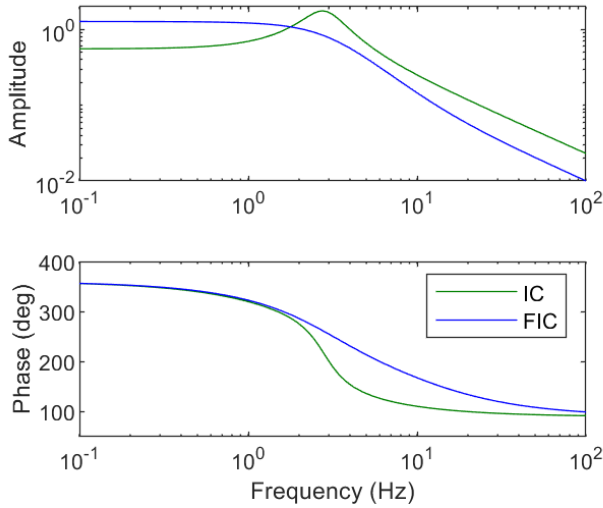


Fig. 4. The impulse frequency response shows that the proposed controller and a traditional impedance controller have similar cut off frequencies at about 2Hz, which could have been expected since they shared the same gains. However, the proposed method behaves as a critically damped system, while the traditional impedance controller is under-damped.

The controller gains used in the experiment are reported in Table I. It shall be noted that the gains of the FIC_{SHE} have been used with both controllers as safety mechanism. However, the safety mechanism was never triggered during our experiments.

A. Results

The impulsive response of the two controllers is portrayed in Figure 4. The system cut-off frequency is about 2Hz in both controllers. The FIC has a critically damped behaviour while the regular impedance controller has an under-damped

TABLE I. Controller Parameters

	Master	Slave	
	FIC	FIC	IC
$K_c^{linear} (N/m)$	0	100	100
$K_c^{angular} (N/rad)$	0	5	5
$D^{linear} (Ns/m)$	2.5	2.5	20
$D^{angular} (Ns/rad)$	0	1.25	1.25
$x_B^{linear} (m)$	0.075	0.075	NA
$x_B^{angular} (rad)$	1.0472	1.0472	NA

FIC: Fractal Impedance Control, IC: Impedance Control. Where x_B is the vector of the force saturation boundaries and $K_{Max} = K_c$, described in section I

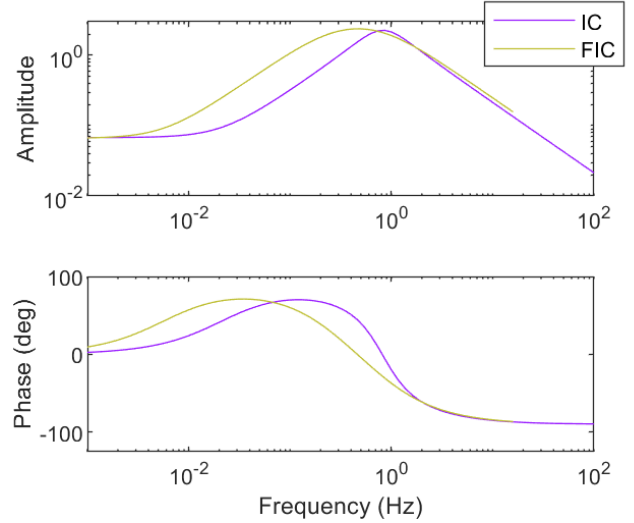


Fig. 5. The spectral analysis of the teleoperation setup recorded for the interaction with the 5 objects in Figure 3 shows that the proposed method has a broader band-pass behaviour, centred on the 2Hz frequency.

behaviour. Figure Figure 5 also confirms these characteristics. However, we also observe a band-pass behaviour due to the user driving the robot using the master device until the slave's end-effector makes contact with the environment, which filters the lower frequencies. It can also be observed how the band-pass is wider where the slave is driven using the FIC controller. Figure 6 compares the behaviour of the two controllers when interacting with different objects. The data show that the transient behaviour of the proposed method is more variable, and it has a lower attenuation of the input signal.

IV. DISCUSSION

The results show that the proposed method has a cut-off frequency similar to the traditional impedance controller, and an intrinsic adaptability to external environments even without gain adaptation (Figure 6). Nevertheless, the FIC also has online gain adaptation capabilities as reported in [21]. The spectral analysis in Figure 5 shows that the proposed method has a wider band-pass when driven by the user, confirming together with the consistently lower attenuation of the inputs a higher transparency compared to the traditional impedance controller.

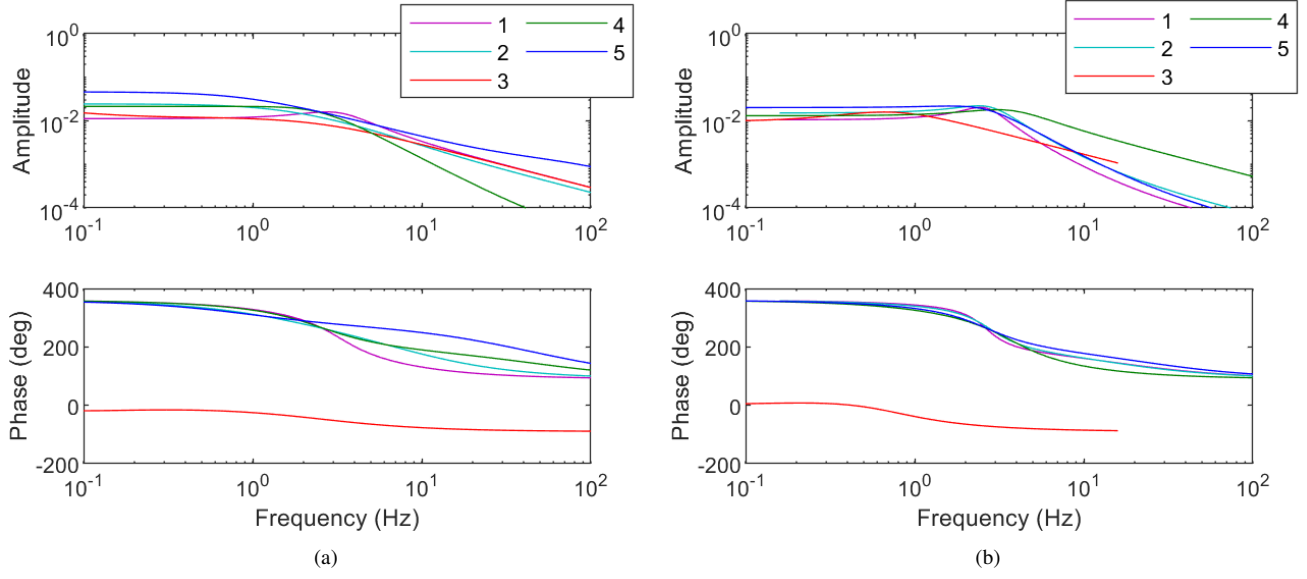


Fig. 6. Separating the data in Figure 5 based on the object interaction. (a) Shows the FIC's higher band-pass is due to its ability to synchronise its behaviour with the environment. (b) Shows the less variable frequency spectrum of the IC.

To better visualise the benefit of such behaviour during haptic interaction, we tested the two controllers in a sequence of dexterous tasks. These tests are not presented as results because they have been conducted using a single skilled operator which had knowledge of the controller being used. The operator was only allowed a single attempt for each task and the choice of the starting controller was alternated to mitigate the operator learning bias. The chosen tasks are:

- i) Removing the lid from the metal box in Figure 3e
- ii) Pushing a golf ball to an end-goal on a rough terrain (sand, gravel, rocks)
- iii) Driving a pile through the sand
- iv) Diving the sponge in Figure 3c through a course
- v) Press an E-stop button on a control panel

The completion times are reported in Table II. The outcome qualitatively shows that the proposed method is more reliable than a traditional impedance controller. The proposed controller succeeded in all the tasks as shown in Figure 7. Traditional impedance control achieved pushing the golf ball, driving the sponge, and pressing E-stop button. The driving task failed to a poorer movement accuracy, while the lid removal failed due to the Franka's safety constraints being triggered.

TABLE II. Task Completion Times (s)

Task	FIC	IC
i	34	NA
ii	26	32
iii	22	NA
iv	94	152
v	6	32

The experimental results show that the proposed method has intrinsic adaptability to different environmental dynamics, even without performing an online gain tuning. Such

characteristics, based on our preliminary analysis, provide the user with better interaction dexterity. Future work will explore more in-depth the haptics performance of the proposed method. Mainly by taking advantage of the presence of the FIC_{SHE} and the online impedance tuning provided by the FIC framework, [21], to improve the framework dexterity capabilities.

APPENDIX I FRACTAL IMPEDANCE CONTROL

The fractal impedance control is a passive controller which has been proposed in [21]. It has variable anisotropic state-dependent stiffness, driving the following dynamics at the end-effector as follows:

$$\Lambda_c \ddot{x} - D_c \dot{x} + K(\tilde{x}, \text{sgn}(\dot{\tilde{x}}))\tilde{x} = 0 \quad (4)$$

where Λ_c is the task-space inertia, D_c is a constant damping, $K(\tilde{x}, \text{sgn}(\dot{\tilde{x}}))$ is the anisotropic state-dependant impedance profile, and $\text{sgn}(\dot{\tilde{x}})$ is the sign of the end-effector velocity which is used to discriminate if the controller is either in convergence or divergence phase.

The stiffness profile $K(\tilde{x}, \text{sgn}(\dot{\tilde{x}}))$ is determined as follows:

Divergence Phase ($\text{sgn}(\dot{\tilde{x}}) = \text{sgn}(\tilde{x})$ or $\dot{\tilde{x}} = 0$):

$$K(\tilde{x}, \text{sgn}(\dot{\tilde{x}})) = K_c + K_v(\tilde{x}) \text{ where}$$

$$K_v(\tilde{x}) = \begin{cases} \frac{W_{\max}}{|\tilde{x}|} - K_c, & \text{if } K_d > K_{\max} \\ e^{(\beta\tilde{x})^2}, & \text{otherwise} \end{cases} \quad (5)$$

Convergence Phase ($\text{sgn}(\dot{\tilde{x}}) \neq \text{sgn}(\tilde{x})$):

$$K(\tilde{x}, \text{sgn}(\dot{\tilde{x}})) = \left(\frac{4}{\tilde{x}_{\max}^2} \right) \int K_d \tilde{x} d\tilde{x} \left(\frac{0.5\tilde{x}_{\max} - \tilde{X}}{\tilde{X}} \right) \quad (6)$$

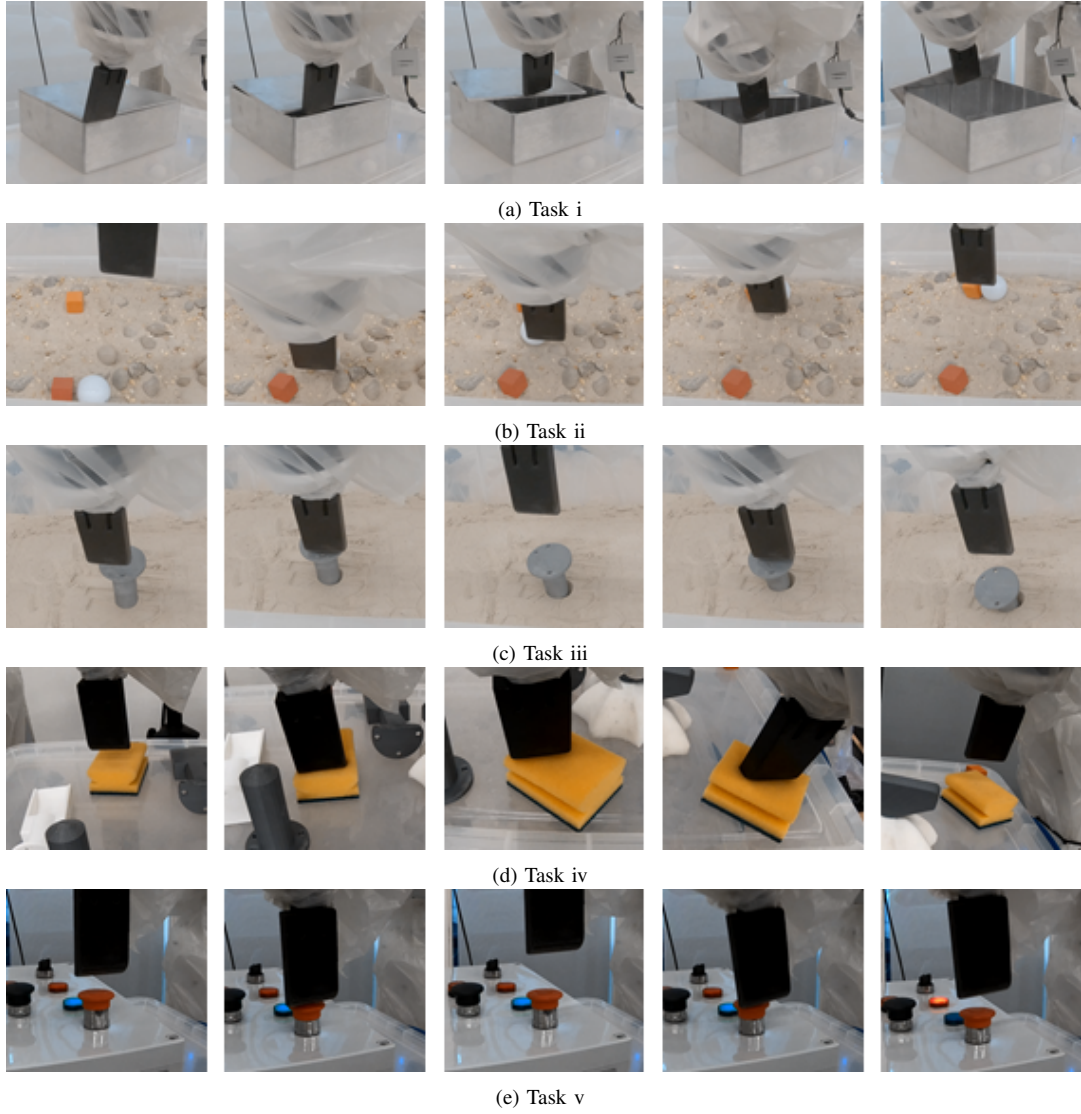


Fig. 7. Snapshots of the 5 tasks from the FIC experiment.

Where K_{const} and K_{var} are the constant and the variable stiffness respectively, W_{max} is the maximum exertable wrench by the robot with respect to its physical limitation, K_{max} is the stiffness upper-bound. \tilde{x}_{max} is the maximum displacement from x_d reached during divergence, and β is adjustable coefficient that controls the stiffness saturation-boundaries.

The upper-bound level for the controller stiffness and β are calculated as follows:

$$\begin{aligned} K_{\text{max}} &= \frac{W_{\text{max}}}{x_B} \\ \beta &= \sqrt{\frac{\ln(K_{\text{max}})}{(x_B)^2}} \end{aligned} \quad (7)$$

where x_B is the pose error set where the controller wrench saturates to W_{max} . The FIC is summarised in algorithm 1.

Algorithm 1: Fractal Impedance Control

```

1 if diverging from  $x_d$  then
2   |  $K(\tilde{x}, \text{sgn}(\dot{\tilde{x}})) \Rightarrow \text{Equation 5}$ 
3 else
4   |  $K(\tilde{x}, \text{sgn}(\dot{\tilde{x}})) \Rightarrow \text{Equation 6}$ 
5 end

```

ACKNOWLEDGMENT

This work has been supported by the following grants: EPSRC UK RAI Hub ORCA (EP/R026173/1), the Future AI and Robotics for Space (EP/R026092/1), and THING project in the EU Horizon 2020 (ICT-2017-1).

REFERENCES

- [1] P. Schmaus, D. Leidner, T. Krüger, A. Schiele, B. Pleintinger, R. Bayer, and N. Y. Lii, "Preliminary insights from the meteron supvis justin

- space-robotics experiment,” *IEEE Robotics and Automation Letters*, vol. 3, no. 4, pp. 3836–3843, 2018.
- [2] P. Schmaus, D. Leidner, R. Bayer, B. Pleintinger, T. Krüger, and N. Y. Lii, “Continued advances in supervised autonomy user interface design for meteron supvis justin,” in *2019 IEEE Aerospace Conference*. IEEE, 2019, pp. 1–11.
 - [3] S. Part, “Impedance control: An approach to manipulation,” *Journal of dynamic systems, measurement, and control*, vol. 107, no. 17, 1985.
 - [4] N. Hogan, “A general actuator model based on nonlinear equivalent networks,” *IEEE/ASME Transactions on Mechatronics*, vol. 19, no. 6, pp. 1929–1939, 2013.
 - [5] Y. Li, G. Ganesh, N. Jarrassé, S. Haddadin, A. Albu-Schaeffer, and E. Burdet, “Force, impedance, and trajectory learning for contact tooling and haptic identification,” *IEEE Transactions on Robotics*, vol. 34, no. 5, pp. 1170–1182, 2018.
 - [6] J. Buchli, E. Theodorou, F. Stulp, and S. Schaal, “Variable impedance control a reinforcement learning approach,” *Robotics: Science and Systems VI*, pp. 153–160, 2011.
 - [7] T. Tsumugiwa, R. Yokogawa, and K. Hara, “Variable impedance control based on estimation of human arm stiffness for human-robot cooperative calligraphic task,” in *Proceedings 2002 IEEE International Conference on Robotics and Automation (Cat. No. 02CH37292)*, vol. 1. IEEE, 2002, pp. 644–650.
 - [8] A. J. van der Schaft and A. Van Der Schaft, *L2-gain and passivity techniques in nonlinear control*. Springer, 2000, vol. 2.
 - [9] J.-H. Ryu, D.-S. Kwon, and B. Hannaford, “Stable teleoperation with time-domain passivity control,” *IEEE Transactions on robotics and automation*, vol. 20, no. 2, pp. 365–373, 2004.
 - [10] N. Hogan and S. P. Buerger, “Impedance and interaction control,” in *Robotics and automation handbook*. CRC press, 2018, pp. 375–398.
 - [11] F. Ferraguti, N. Preda, A. Manurung, M. Bonfe, O. Lamercy, R. Gassert, R. Muradore, P. Fiorini, and C. Secchi, “An energy tank-based interactive control architecture for autonomous and teleoperated robotic surgery,” *IEEE Transactions on Robotics*, vol. 31, no. 5, pp. 1073–1088, 2015.
 - [12] C. Secchi, S. Stramigioli, and C. Fantuzzi, “Position drift compensation in port-hamiltonian based telemanipulation,” in *2006 IEEE/RSJ International Conference on Intelligent Robots and Systems*. IEEE, 2006, pp. 4211–4216.
 - [13] M. Franken, S. Stramigioli, S. Misra, C. Secchi, and A. Macchelli, “Bilateral telemanipulation with time delays: A two-layer approach combining passivity and transparency,” *IEEE transactions on robotics*, vol. 27, no. 4, pp. 741–756, 2011.
 - [14] V. Duindam and S. Stramigioli, “Port-based asymptotic curve tracking for mechanical systems,” *European Journal of Control*, vol. 10, no. 5, pp. 411–420, 2004.
 - [15] T. S. Tadele, T. J. de Vries, and S. Stramigioli, “Combining energy and power based safety metrics in controller design for domestic robots,” in *2014 IEEE International Conference on Robotics and Automation (ICRA)*. IEEE, 2014, pp. 1209–1214.
 - [16] G. Raiola, C. A. Cardenas, T. S. Tadele, T. De Vries, and S. Stramigioli, “Development of a safety-and energy-aware impedance controller for collaborative robots,” *IEEE Robotics and automation letters*, vol. 3, no. 2, pp. 1237–1244, 2018.
 - [17] K. Kronander and A. Billard, “Stability considerations for variable impedance control,” *IEEE Transactions on Robotics*, vol. 32, no. 5, pp. 1298–1305, 2016.
 - [18] C. Schindlbeck and S. Haddadin, “Unified passivity-based cartesian force/impedance control for rigid and flexible joint robots via task-energy tanks,” in *2015 IEEE international conference on robotics and automation (ICRA)*. IEEE, 2015, pp. 440–447.
 - [19] A. Dietrich, C. Ott, and S. Stramigioli, “Passivation of projection-based null space compliance control via energy tanks,” *IEEE Robotics and automation letters*, vol. 1, no. 1, pp. 184–191, 2015.
 - [20] F. Ferraguti, C. Secchi, and C. Fantuzzi, “A tank-based approach to impedance control with variable stiffness,” in *2013 IEEE International Conference on Robotics and Automation*. IEEE, 2013, pp. 4948–4953.
 - [21] K. K. Babarahmati, C. Tiseo, J. Smith, H. C. Lin, M. S. Erden, and M. Mistry, “Fractal impedance for passive controllers,” *arXiv preprint arXiv:1911.04788*, 2019.
 - [22] D. Zhou and K. Tadano, “Relationship between system parameters and operator’s haptic sensation in bilateral controlled master–slave system,” *International Journal of Human–Computer Interaction*, vol. 36, no. 2, pp. 143–155, 2020.